Chem

CellPress

Article

Photo-induced thiolate catalytic activation of inert C_{aryl}-hetero bonds for radical borylation

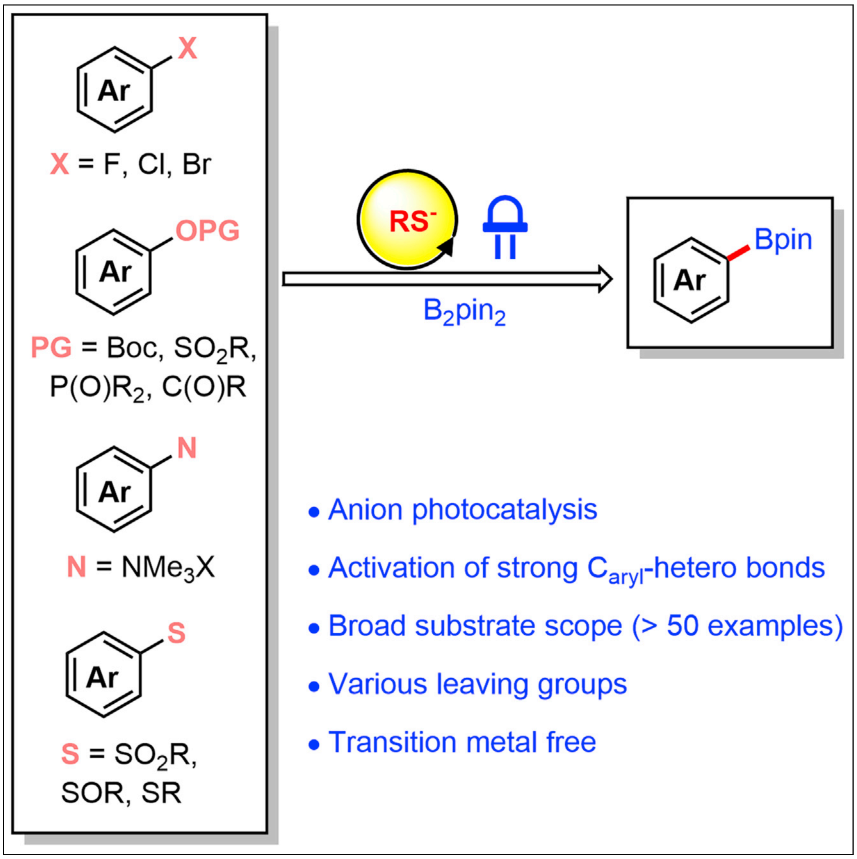

An unprecedented photo-induced thiolate-catalytic strategy for *ipso*-borylation of strong C_{aryl}-hetero bonds has been developed. This approach provides a platform for activation of strong chemical bonds (C–F, C–O, C–X, C–N, and C–S) and their transformation into synthetically valuable boronates for a broad substrate scope with high functional-group compatibility. Mechanistic studies suggest that the unique reactivity of the reaction stems from charge-transfer complex formation between thiolate catalyst and substrates.

Shun Wang, Hua Wang,
Burkhard König

burkhard.koenig@ur.de

Highlights

Highly reducing photocatalytic system

Inexpensive organocatalyst

Borylation of strong C–F, C–O, C–N, and C–S bonds

Various leaving groups and >50 examples

Wang et al., Chem 7, 1653–1665
June 10, 2021 © 2021 Elsevier Inc.
https://doi.org/10.1016/j.chempr.2021.04.016

Chem

CellPress

Article

Photo-induced thiolate catalytic activation of inert C_{aryl}-hetero bonds for radical borylation

Shun Wang,[1] Hua Wang,[1] and Burkhard König[1,2,*]

SUMMARY

Substantial effort is currently being devoted to obtaining photoredox catalysts with high redox power. Yet, it remains challenging to apply the currently established methods to the activation of bonds with high bond dissociation energy and to substrates with high reduction potentials. Herein, we introduce a novel photocatalytic strategy for the activation of inert substituted arenes for aryl borylation by using thiolate as a catalyst. This catalytic system exhibits strong reducing ability and engages non-activated C_{aryl}–F, C_{aryl}–X, C_{aryl}–O, C_{aryl}–N, and C_{aryl}–S bonds in productive radical borylation reactions, thus expanding the available aryl radical precursor scope. Despite its high reducing power, the method has a broad substrate scope and good functional-group tolerance. Spectroscopic investigations and control experiments suggest the formation of a charge-transfer complex as the key step to activate the substrates.

INTRODUCTION

Photoredox catalysis has emerged as a powerful technique in organic synthesis over the past decade through converting the energy of photons into redox potentials for chemical processes. This empowers organic chemists to realize a number of unprecedented chemical transformations under mild conditions for organic synthesis.[1–6] However, the range of attainable redox potentials in a typical photocatalysis system is governed by the energy of the absorbed photon. Intersystem crossing and non-radiative pathways diminished this energy inevitably.[7] Thus, it is challenging to activate high redox power demanding substrates by visible-light irradiation. For instance, reductive transformations, particularly those that require highly reducing power, remain an underdeveloped field. To this end, considerable efforts have been devoted toward the development of new photocatalytic systems with a high reduction ability over the past few years. To overcome the thermodynamic limits, several approaches to accumulate the energy of two or more photons enhancing the reducing power of a photocatalyst have been established.[7–10] We have reported a consecutive photo-induced electron transfer (conPET) utilizing two photons via excitation of photogenerated radical anions (Scheme 1A, equation 1).[11–13] Likewise, photoexcitation of electrochemically generated radical anions was shown to be capable of generating high reduction power.[14,15] Nicewicz et al. showed that the acridine radical ACR• could act as an extremely potent photoreductant upon excitation with light (Scheme 1A, equation 2).[16] Moreover, direct photoexcitation of an organo-anionic species has been demonstrated to provide exciting opportunities to access highly reducing reactive intermediates (Scheme 1B).[10,17,18]

Arylboronates are recognized as essential building blocks in organic synthesis, material science, and drug discovery.[19,20] Transition-metal-catalyzed Miyaura

The bigger picture

Cross-coupling reactions are essential tools in the modern synthesis of drugs, natural products, and materials. The recent developments in photocatalytic radical generation have improved and expanded the classic metal-catalyzed cross-coupling reactions even further. However, sp^2 cross-coupling reactions require aryl halides or related active leaving groups, such as triflates. Substituted arenes bearing strong C–X bonds remain inert to current methods. Now, we describe a new thiolate photocatalysis for the activation of inert substituted arenes in *ipso*-borylation reactions. This catalytic system exhibits strong reducing power and allows the borylation of stable C_{aryl}–F, C_{aryl}–O, C_{aryl}–N, and C_{aryl}–S bonds, which are considered chemically stable at mild reaction conditions. Our method considerably widens the available substrate scope of aryl radical precursors, and we anticipate that this report will inspire new chemistry based on inert chemical bond activation.

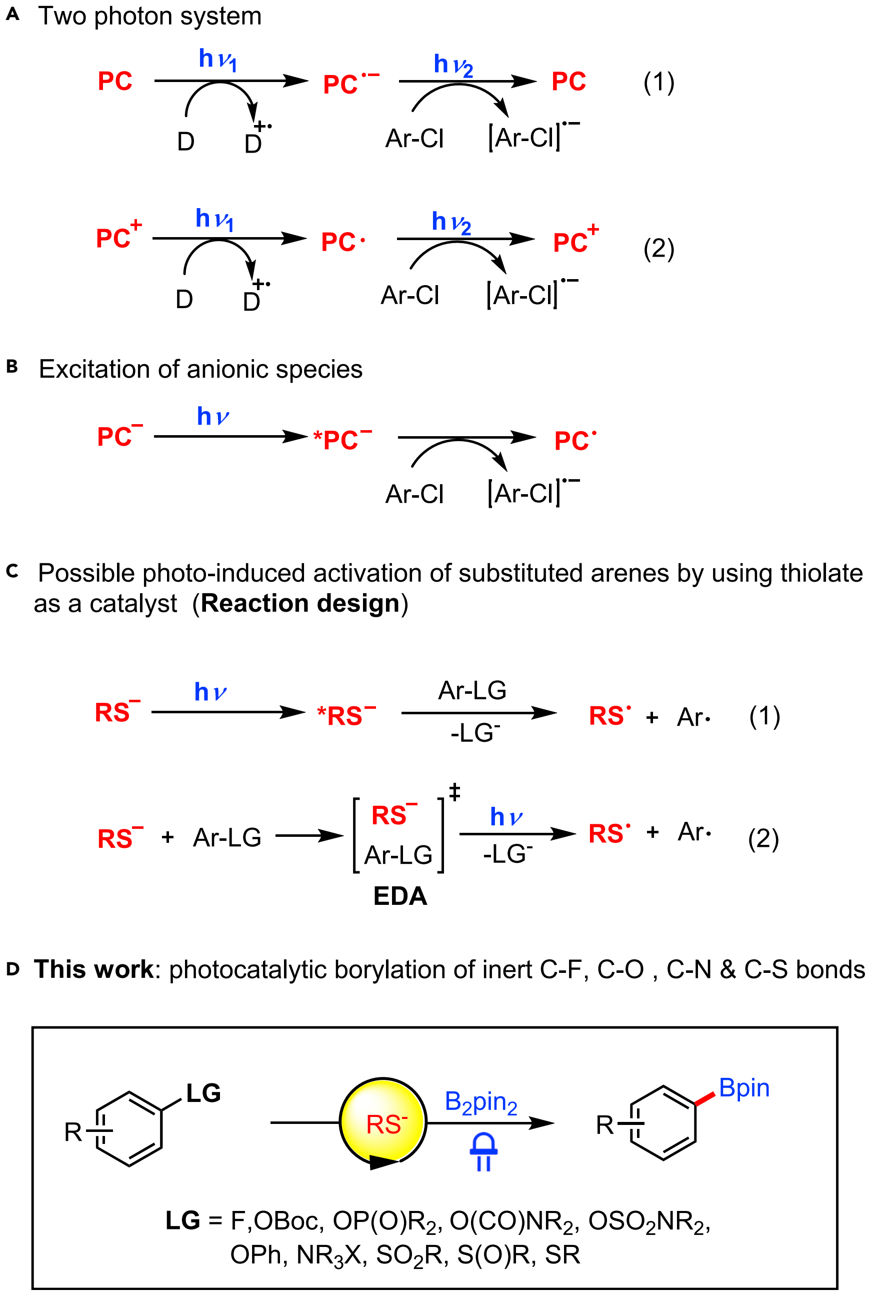

Scheme 1. Photocatalytic strategies for accessing high reduction power for SET activation of substituted arenes

borylation of aryl halides has been developed as one of the most efficient methods for synthesizing arylboron reagents.[21,22] In recent years, photocatalytic borylation has attracted considerable research interest and opened a new avenue to access arylboronates.[23–27] A number of photo-induced systems that allow for the borylation of aryl-X bonds from a wide range of substrates, such as aryldiazonium salts,[28–30] aryl ammonium salts,[31,32] aryl (pseudo) halides,[15,31–41] and redox-active esters,[42] have been developed. However, most established photo-induced borylation methods are limited to substrates with labile aryl-hetero bonds or low reduction potentials.

---

[1] Institute of Organic Chemistry, Faculty of Chemistry and Pharmacy, University of Regensburg, 93040 Regensburg, Germany

[2] Lead contact

*Correspondence: burkhard.koenig@ur.de

https://doi.org/10.1016/j.chempr.2021.04.016

Thus, it remains highly challenging to apply the current methods to the borylation of inert bonds, such as unactivated C_{aryl}–F, C_{aryl}–O, C_{aryl}–N, and C_{aryl}–S bonds, because of their high bond dissociation energy and high reduction potentials of substrates. The development of a strategy for the borylation of these bonds would not only greatly widen the available substrate types to access arylboronates but also might represent a significant step toward utilizing unreactive bonds as functional groups in cross-coupling reactions.

Continuing our research in exploring the reducing ability of anionic species in photoredox catalysis,[43,44] we wondered whether we could generate aryl radicals from inert bonds (C_{aryl}–F, C_{aryl}–O, C_{aryl}–N, and C_{aryl}–S bonds) for borylation by using a sulfur-centered anion (e.g., thiolate) as a photocatalyst. The proposed catalytic system was inspired by our previous finding wherein thiolate could efficiently shuttle electrons from the boronate radical anion, a species that is produced in radical borylation processes, to the photocatalytic system.[45] It was therefore hypothesized that using thiolate directly as a photocatalyst might offer an exciting opportunity for the activation of inert C_{aryl}–X bonds to generate aryl radicals. In the anticipated activation of substituted arenes by thiolate photocatalysis, two possible reaction modes might be involved as shown in Scheme 1C: (1) direct interaction of substituted arenes with the excited state of thiolate and (2) the formation of a charge-transfer complex between thiolate catalyst and substituted arenes.[46–58] We report herein the successful application of thiolate catalysis for the photo-induced borylation of substituted arenes through the cleavage of non-activated C(sp^2)–F, C(sp^2)–O, C(sp^2)–N, and C(sp^2)–S bonds (Scheme 1D).

RESULTS AND DISCUSSION

Investigation of reaction conditions

We commenced the study by evaluating the defluoroborylation reaction of fluorobenzene **1a** with B_2pin_2 (bis(catecholato)diboron). As a result of the high bond dissociation energy (BDE) of Ar–F bonds (e.g., the BDE of Ph–F bond is 526 $kJ \cdot mol^{-1}$), only a few examples are available for the borylation of unactivated aryl fluoride under transition-metal-free conditions at present.[31,37,59] To our delight, the desired borylated product **2a** was obtained in 33% yield at room temperature by irradiation with a 385–390 nm LED with CsF as a base and sodium 3-methyl-phenyl thiolate (30% mol) as the catalyst (Table 1, entry 1; Figure S1). Studies with other thiolates revealed that pyridine-2-thiolate (2-PySNa) is the optimal catalyst yielding the product in 56% yield (entries 2–4). It is worth mentioning that sodium cyclohexanethiolate (CySNa) and sodium 1-adamantanethiolate (1-AdSNa) showed comparably good catalytic performances affording the product, whereas pyridine as a catalyst did not give the product (entry 5), thus indicating that in our reaction the reactivity stems from the thiolate under photocatalytic conditions. Changing the solvent from MeCN to dimethyl sulfoxide (DMSO) or tetrahydrofuran (THF) gave either a poor yield or trace amount of the product (entry 6 and 7). To further increase the yield, we examined a variety of bases. Tetramethylammonium fluoride (TMAF) turned out to be the optimal base, resulting in the formation of **2a** in 74% yield; the increased reactivity was most likely a result of its superior solubility in MeCN (entry 8). Using other bases, such as KF, Cs_2CO_3, and CsOAc, failed to improve the yield (entries 9–11). In the absence of base, the reaction afforded **2a** in only 13% yield (entry 12). To our delight, the yield was further improved to 81% when slight excess amounts of B_2pin_2 and TMAF were employed (entry 13). The use of the more Lewis-acidic diboron source B_2cat_2 afforded only a trace amount of compound **2a** (entry 14). Control experiments showed that both thiolate catalyst 2-PySNa and light irradiation (385–390 nm) were

Table 1. Evaluation of reaction conditions for the borylation of fluorobenzene with B_2pin_2

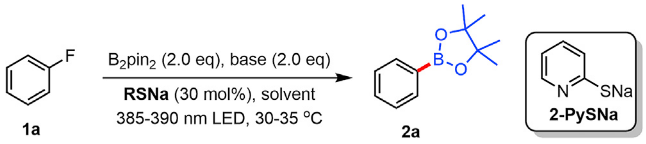

1a

2a

Entry	Base	Catalyst	Solvent	Yield[a]
1	CsF	3-Me-PhSNa	MeCN	33%
2	CsF	CySNa	MeCN	48%
3	CsF	1-AdSNa	MeCN	40%
4	CsF	2-PySNa	MeCN	56%
5	CsF	pyridine	MeCN	n.d.
6	CsF	2-PySNa	DMSO	24%
7	CsF	2-PySNa	THF	trace
8	TMAF	2-PySNa	MeCN	74%
9	KF	2-PySNa	MeCN	19%
10	Cs_2CO_3	2-PySNa	MeCN	33%
11	CsOAc	2-PySNa	MeCN	27%
12	–	2-PySNa	MeCN	13%
13[b]	TMAF	2-PySNa	MeCN	81% (78%),[c] 70%[d]
14[e]	TMAF	2-PySNa	MeCN	trace[f]
15[g]	TMAF	2-PySNa	MeCN	n.d.
16[h]	TMAF	2-PySNa	MeCN	trace
17[i]	TMAF	2-PySNa	MeCN	10%

Reaction conditions: **1a** (0.2 mmol), B_2pin_2 (0.4 mmol), base (0.4 mmol), and catalyst (30 mol %) in 2 mL of solvent under irradiation with a 385–390 nm LED (3.8 W) at 30°C–35°C (internal temperature) for 24 h under N_2 atmosphere. n.d., not detected; TMAF, tetramethylammonium fluoride; B_2pin_2, bis(pinacolato)diboron; CySNa, sodium cyclohexanethiolate; 1-AdSNa, sodium 1-adamantanethiolate; 2-PySNa, pyridine-2-thiolate; B_2cat_2, bis(catecholato)diboron.

[a] Yields were determined by GC-FID analysis of the crude reaction mixture with n-dodecane as an internal standard.

[b] B_2pin_2 (3.0 equiv), TMAF (3.0 equiv).

[c] Isolated yield.

[d] 6 mmol scale.

[e] B_2cat_2 in place of B_2pin_2.

[f] Work up with Et_3N (0.5 mL) and pinacol (0.8 mmol).

[g] 455 nm LED.

[h] In the dark.

[i] No 2-PySNa.

essential for this reaction (entries 15–17). This method is easily scalable such that boronic ester **2a** can be obtained in 70% yield on a 6 mmol scale (Figure S2).

Scope of leaving group for *ipso*-borylation

Encouraged by these results, we next turned our attention to test the feasibility of this catalytic system with arene substrates bearing different leaving groups (Scheme 2). When the same reaction was attempted with chlorobenzene **1b** (E^{P}_{red} = -2.78 V versus saturated calomel electrode [SCE]) and bromobenzene **1c** (E^{P}_{red} = -2.44 V versus SCE), borylation product **2a** was obtained in 74% and 78% yield, respectively. We then focused on the borylation of C–O bonds of phenol derivatives considering that phenols have emerged as versatile and cost-efficient alternatives to aryl halides.[25,60,61] It is worthwhile to note that, unlike the use of reactive aryl sulfonates such as aryl triflates, mesylates, or tosylates, only a few methods are known for the catalytic radical borylation of less or even non-activated aryl esters as coupling partners via C–O bond cleavage.[25,32,40] In particular, using slightly modified reaction conditions (Table S2) borylated O-Boc-protected phenol **1d** efficiently to give product **2a** in 65% yield. To the best of our knowledge, this is the first example of transition-metal-free borylation of aryl carbonates via C–O bond cleavage.

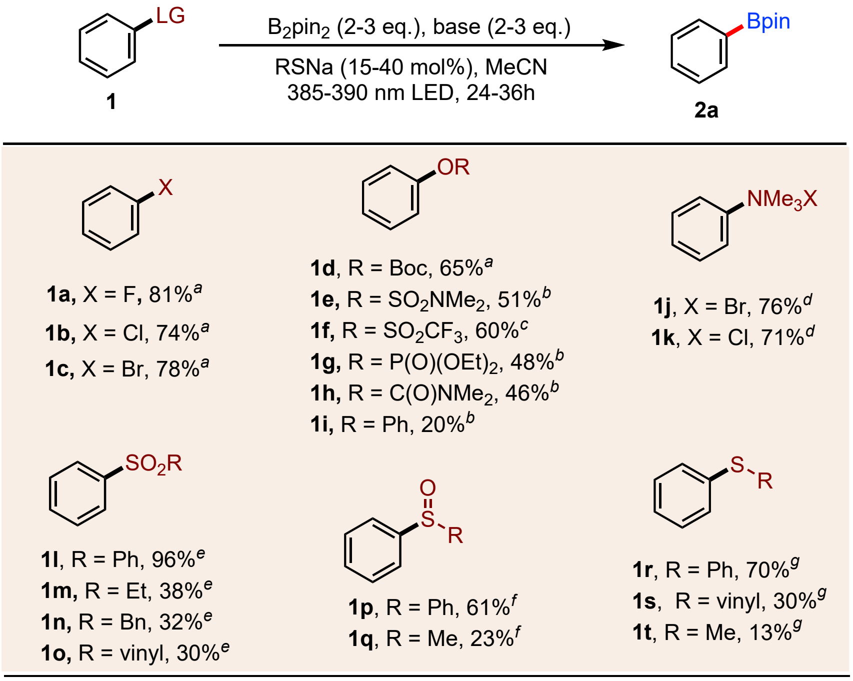

Scheme 2. Leaving-group scope for photo-induced *ipso*-borylation of substituted arenes

Reaction condition: **1** (0.2 mmol), B_2pin_2 (3.0 equiv), base (3.0 equiv), and 2-PySNa (15%–40% mol) in 2 mL of MeCN under irradiation with a 385–390 nm LED (3.8 W) at 30–35°C for 24 h under N_2 atmosphere. Yields were determined by GC-FID using n-dodecane as an internal standard.[a]CsF (3.0 equiv), 2-PySNa (40 mol %), 36 h.[b]TMAF (3.0 equiv), MeCN (1.5 mL), 36 h.[c]CsOAc (3.0 equiv), AcSK (20 mol %).[d]KOAc (3.0 equiv), 2-PySNa (15 mol %), MeCN (1.5 mL).[e]CsF (3.0 equiv), 1-AdSNa (30 mol %).[f]B_2pin_2 (2.0 equiv), CsF (2.0 equiv), CySNa (30 mol %).[g]B_2pin_2 (2.0 equiv), CsF (2.0 equiv), 1-AdSNa (30 mol %).

Furthermore, we found that the reaction system was feasible for sulfamate **1e**, triflate **1f**, phosphate **1g**, and carbamate **1h**. Interestingly, even the C–O bond of diphenylether showed a certain degree of reactivity in the reaction. Arylammonium salts **1j** and **1k** were also viable for this transformation, leading to C–N borylated products in 76% and 71% yield, respectively.

Given that organosulfur compounds are widely present in natural products, drugs, and proteins, our protocol was briefly examined as a viable route for the C–S bond borylation of sulfur-containing molecules, which allows modification of their structures.[62–64] Indeed, the C–S bond of diphenyl sulfone **1l** ($E^p_{red} = -2.06$ V versus SCE) could be borylated to give product **2a** in excellent yield. When alkyl phenyl sulfones (**1m** and **1n**) and vinyl phenyl sulfone **1o** were used, the borylation occurred selectively at the phenyl-SO_2 bonds to give aryl boronic ester product **2a**, whereas the alkyl boronic esters were merely observed in trace amounts. The reactivity is in contrast to Nambo and Crudden's observation, wherein the borylation of alkyl phenyl sulfones occurred predominately to afford alkyl boronic esters in a pyridine catalytic system.[65] Other than sulfones, our strategy permitted the use of diphenyl sulfoxide **1p** ($E^p_{red} = -2.42$ V versus SCE) and methyl phenyl sulfoxide **1q** ($E^p_{red} = -2.58$ V versus SCE) as the phenyl radical precursors for borylation, albeit the reaction in the latter case proceeds with lower efficiency. Subsequently, we were glad to find that this methodology was applicable to convert aryl sulfides to aryl boronic esters through C–S cleavage. Specifically, diphenyl sulfide **1r** ($E^p_{red} = -2.8$ V versus SCE) reacted smoothly to give **2a** in a 70% yield, whereas vinyl phenyl sulfide

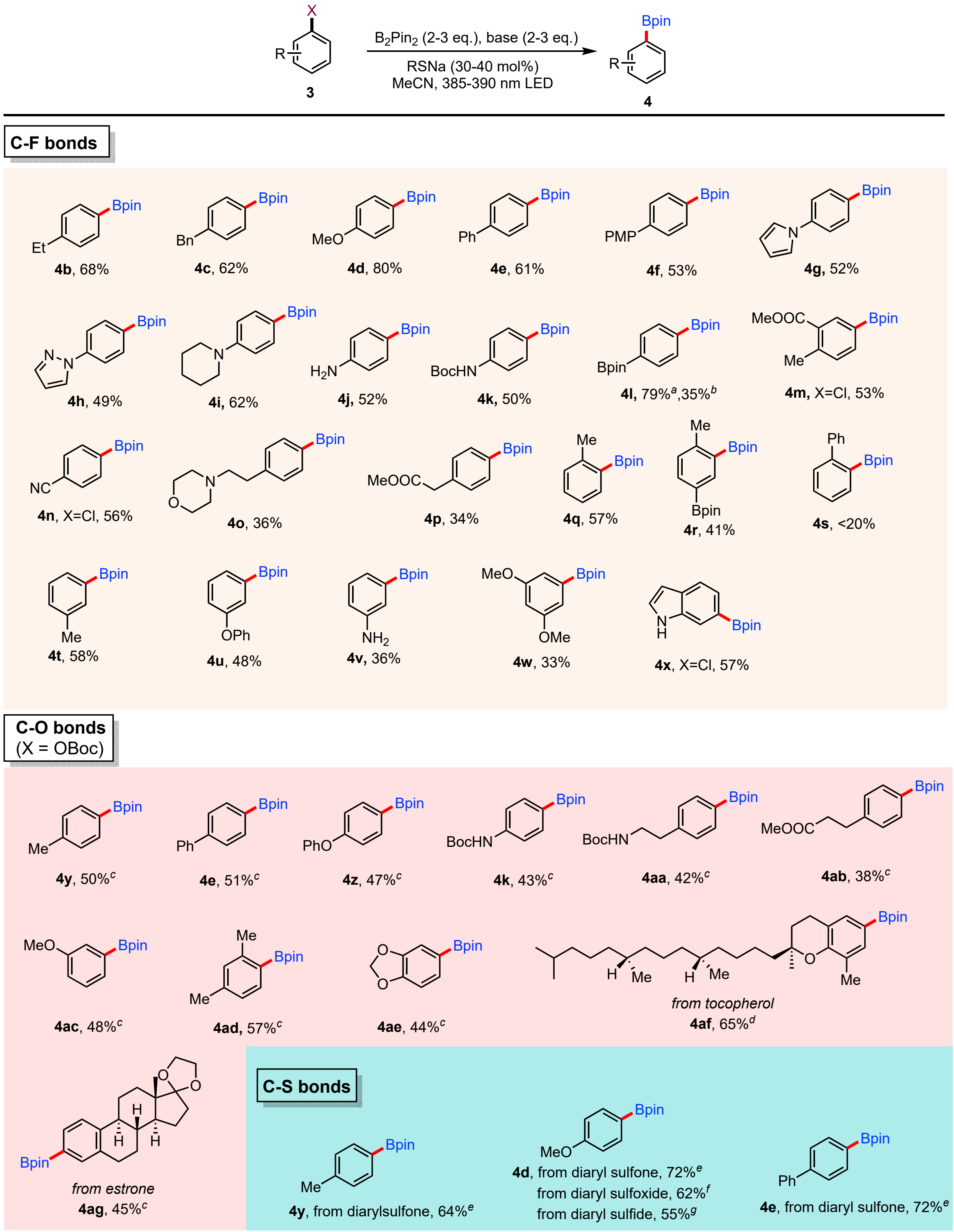

Scheme 3. Substrate scope for photo-induced *ipso*-borylation

Scheme 3. *Continued*

Reaction conditions: **3** (0.2 mmol), B_2pin_2 (3.0 equiv), TMAF (3.0 equiv), and 2-PySNa (30% mol) in 2 mL of MeCN under irradiation with a 385–390 nm LED (3.8 W) at 30°C–35°C for 24 h under N_2 atmosphere. Isolated yields are shown.[a]CsF (3.0 equiv), B_2pin_2 (3.0 equiv).[b]From 1,4-difluorobenzene, TMAF (4.0 equiv), B_2pin_2 (4.0 equiv), mono-borylation product was obtained in 25% yield.[c]CsF (3.0 equiv), 2-PySNa (40 mol %), 36 h.[d]X = OSO2NMe2, 2-PySNa (40% mol), MeCN (1.5 mL).[e]CsF (3.0 equiv), 1-AdSNa (30 mol %).[f]CsF (2.0 equiv), B_2pin_2 (2.0 equiv), CySNa (30 mol %).[g]CsF (2.0 equiv), B_2pin_2 (2.0 equiv), 1-AdSNa (30 mol %).

demonstrated diminished reactivity. An attempt to borylate thioanisole **1t** was unsuccessful in that it afforded the target product **2a** in 13% yield. These results are particularly noteworthy given that thiolate anions are rarely used as leaving groups in radical arylation reactions and that sulfides possess more negative reduction potentials, which are caused by the electron-donating property of SR groups.[8,66]

Substrate scope for the borylation of C–X, C–O, and C–S bonds

After surveying the scope of phenyl radical precursors, we next sought to study the preparative scope of our reaction by utilizing substituted aryl fluorides and chlorides, O-Boc-protected phenols, and organosulfur compounds (Scheme 3). We were pleased to see a wide variety of aryl fluorides bearing *para*-(**3b–3p**), *ortho*-(**3q** and **3r**), and *meta*-(**3t–3v**) substituents reacting smoothly to afford the corresponding boronic esters. A broad range of substituents at the *para*-position—including strongly electron-donating groups, such as –OMe (**3d**), piperidinyl (**3i**), and $–NH_2$ (**3j**), and electron-neutral ethyl (**3b**), benzyl (**3c**), and boronic ester (**3l**) groups—were all tolerated and provided the desired products in good yields. The presence of acidic protons in amine (**3j** and **3v**) and amide (**3k**) did not interfere with the reaction. Aromatic substituents, such as aryl (**3e** and **3f**), pyrrole (**3g**), and pyrazole (**3h**), were compatible with the reaction conditions. The use of aryl fluorides bearing electron-withdrawing groups (EWGs) (e.g., acetyl, CN, and CF_3) afforded the products in low yields, although the starting materials were completely consumed under the reaction conditions. However, corresponding arylchlorides bearing strong EWGs (e.g., COOMe and CN) were tolerated in the reaction system and delivered the desired products **4m** and **4n** in moderate yields. This observation might be attributed to the strong electron-withdrawing property of fluoro substituents, which leads to the over-reduction of substrates bearing other EWGs on the aromatic ring. Substrates bearing functional groups such as morpholine and ester on the alkyl chains were tolerated (**3o** and **3p**). *ortho*-Methyl-substituted aryl fluorides **3q** and **3r** reacted smoothly to provide the products in 57% and 41% yields, respectively, whereas more sterically hindered phenyl groups at the *ortho*-position inhibited the reactivity such that the hydrodefluorination product was detected as the major byproduct. Meta-substituted aryl fluorides bearing various functional groups, such as phenoxy and amine, showed good reactivity in the reaction conditions. Aryl fluoride bearing two methoxy groups also reacted to furnish the corresponding product (**4w**) in 33% yield, highlighting the high reactivity of the catalytic system. In addition, an unprotected indole functionality was preserved in the borylation process. It should be noted that hydrodehalogenation products were detected as the main side products in most cases as a result of a competing hydrogen atom transfer (HAT) pathway (Schemes S1 and S2).

Prompted by these results, we proceeded to explore the scope of the *ipso*-borylation of Ar–OBoc and Ar–S bonds. We were delighted to find that many synthetically useful functional groups, including alkyl (**4y** and **4ad**), phenyl (**4e**), phenoxy (**4z**), amide (**4k**), and alkoxy (**4ac** and **4ae**) substituents on the phenyl ring of Boc-protected phenols, could be tolerated and provided the products in moderate yields. These results are noteworthy considering that the electron-rich Boc-protected phenols should possess very negative reduction potentials. Moreover, amide **4aa** and ester **4ab** functionalities on the alkyl chain of the phenolic compounds remained untouched in the reaction conditions. The synthetic utility of this chemistry was further demonstrated by the successful borylation of a δ-tocopherol and estrone derivatives, affording the products **4af** and **4ag** in 65% and 45% yields, respectively. Likewise, we observed hydrodefunctionalized products as the major side products for the borylation of Boc-protected phenols. In these cases, we observed lower conversions than with the fluoroarenes results (Scheme S3). Finally, the borylation of diarylsulfones bearing methyl, methoxy, and phenyl groups was fruitful in giving 64%–72% product yields of the isolated boronic esters (**4y**, **4d**, and **4e**). Moreover, methoxy-substituted diaryl sulfoxide and sulfide were also suitable substrates for borylation.

Mechanistic insights

To obtain mechanistic insights into the reaction mechanism, we carried out a number of experimental studies. At the outset, the effect of radical scavengers on the current borylation system was examined (Scheme S5; Figure 1A). The presence of 1,1-DPE (1,1-diphenylethylene) inhibited the reaction completely, and the corresponding trapping adducts were formed in 5% yield. When aryl fluoride **3ah** with an *ortho*-allyloxy side chain was subjected to the standard conditions, cyclic alkylboronate **4ah** derived from a radical addition-borylation sequence was detected in 13% yield. These results collectively suggest the intermediacy of the phenyl radical in the reaction. To elucidate the radical generation process, we conducted further control experiments. Under light irradiation (385–390 nm), fluorobenzene **1a** reacted with 2-PySNa to give benzene, disulfide, and sulfide, albeit in low conversion (16%), whereas no reaction could be observed in the dark (Figure 1B, equations 1 and 2). These results imply that phenyl radical and thiyl radical could be generated through direct photo-induced electron transfer between the thiolate and fluorobenzene with low efficiency.

Next, we performed UV-visible (UV-vis) spectroscopic measurements of reaction components to explore the electron transfer process between 2-PySNa and **1a**. It turned out that absorption spectra of B_2pin_2, substrate **1a**, and TMAF showed bands exclusively in the UV region (<300 nm) (Figure S10). However, 2-PySNa was observed to absorb light at 390 nm, and the addition of B_2pin_2 (1.0 equiv) led to a clear redshift by ~50 nm in absorption. A further significant redshift appeared when TMAF and **1a** were added to the mixture of 2-PySNa and B_2pin_2, whereas this signal change was not observed in the absence of TMAF (Figure 1C). Likewise, obvious redshifts were observed in the mixture of 2-PySNa, B_2pin_2, and TMAF (or CsF) with other types of substrates (**1b–1h**) (Figures S11–S17). In contrast, new absorption bands were directly observed when **1j**, **1l**, **1p**, or **1r** was mixed with the corresponding optimal thiolate (Figures S18–S21). These results might support the formation of charge-transfer complexes in the reaction processes.[67,68]

Moreover, we were intrigued by the redshift in the UV-vis spectrum of 2-PySNa after the addition of B_2pin_2. ^{11}B NMR spectroscopic analysis revealed that a new peak with a chemical shift of 8.8 ppm appeared when B_2pin_2 was mixed with 2-PySNa, suggesting the formation of an anionic diboron species (Figure S24). Meanwhile, both the ^{1}H NMR and ^{13}C NMR signals of 2-PySNa were shifted after 1.0 equiv of B_2pin_2 was added, confirming the formation of a new boryl species (Figures S25 and S26). Considering the ease with which diboronate esters can react with pyridine type bases to form the corresponding Lewis base adducts,[42,69–71] we postulated that a Lewis acid-base adduct formed between 2-PyS^- and B_2pin_2 was responsible for the observed redshift.

To study the photo-induced electron-transfer process between substrates and thiolate catalysts, we conducted a series of control experiments using substrates **1** and

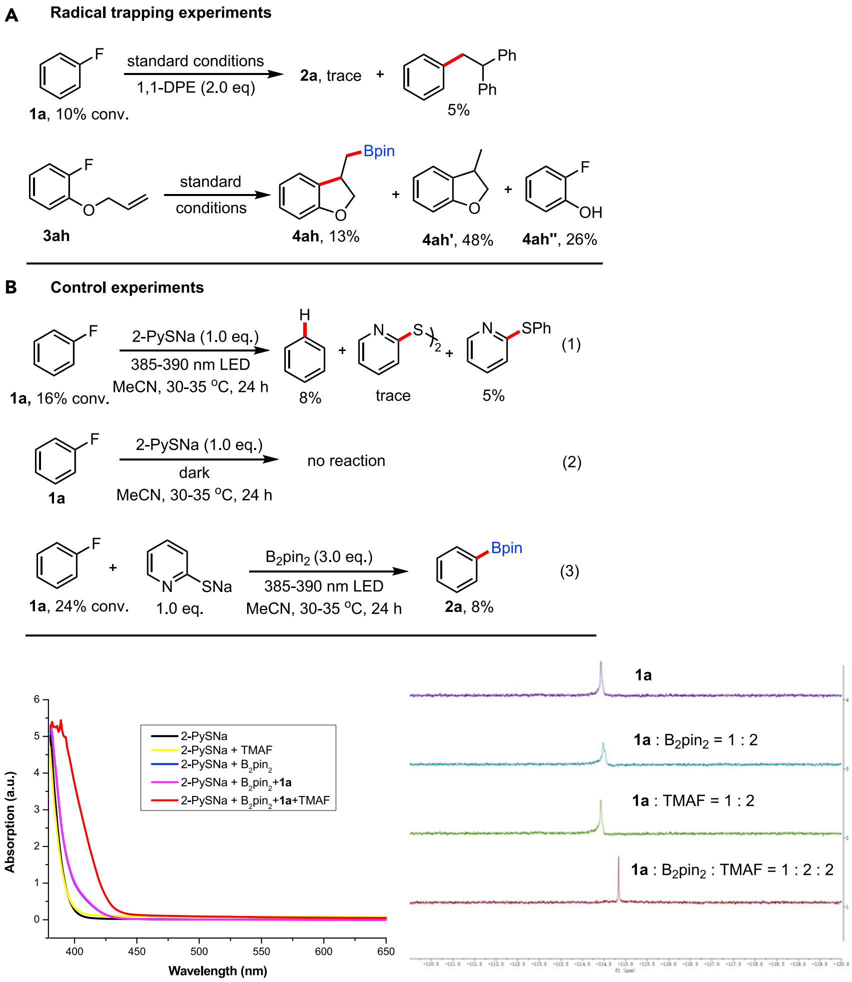

Figure 1. Mechanistic studies

(A) Radical trapping experiments.

(B) Control experiments to elucidate the mechanism.

(C) UV-vis spectra of reaction components.

(D) ^{19}F NMR spectra of **1a** in the presence of B_2pin_2 and/or TMAF.

thiolates as reactants (Schemes S7–S18). First, thiolates could react with substrates **1j**, **1p**, and **1r**, which can directly form an electron donor-acceptor (EDA) complex with them, to afford benzene in high yields under light irradiation (Schemes S15, S17, and S18). Subsequent control experiments demonstrated that in the absence of fluoride, a low conversion of **1a** (24%) and only 8% borylation product **2a** were observed with 1.0 equiv of 2-PySNa (Figure 1B, equation 3). Similarly, reactions of **1b–1h** and **1l** with 2-PySNa (1.0 equiv) gave low conversions (Schemes S8–S14 and S16) under light irradiation. We thus suspect that it is very likely that the activation of substrates by the co-existence of fluoride and B_2pin_2 could facilitate the single-electron transfer (SET) between thiolate and **1a–1h**.

Subsequently, we chose fluorobenzene **1a** as the model substrate to study the potential activation effect by fluoride and B_2pin_2. We first observed a C–F chemical shift moving upfield from −114.51 to −114.84 ppm after mixing **1a** with 2.0 equiv of B_2pin_2 and TMAF, whereas the C–F chemical shift was not affected by B_2pin_2 or

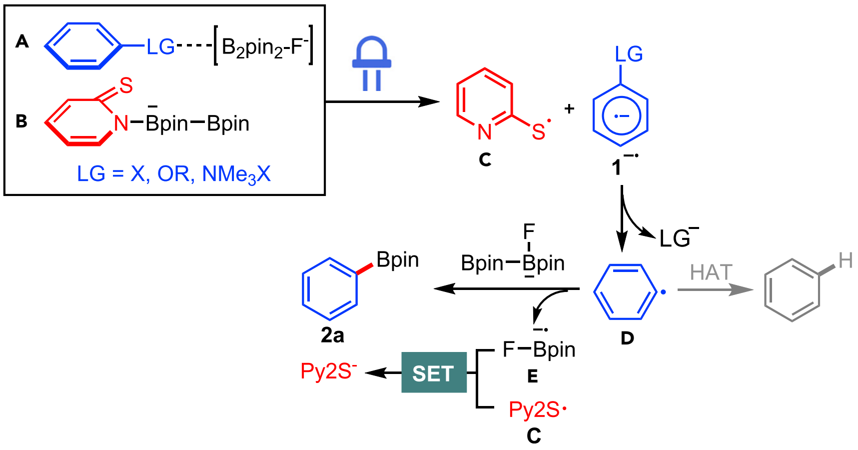

Scheme 4. Mechanistic proposal

TMAF separately (Figures 1D and S28). On the other hand, we observed the formation of a sp^2–sp^3 fluoride diborane adduct between TMAF and B_2pin_2 by ^{19}F NMR measurements (Figure S28).[39,72,73] We thus propose that an *in-situ*-generated nucleophilic boryl anion species $[B_2pin_2\text{-}F^-]$ could activate fluorobenzene **1a**, facilitating the single electron transfer and subsequent fluoride leaving process. We speculate that this activation effect is also essential for the photo-induced electron-transfer event between substrates **1b**–**1h** or **1l** and the catalyst to occur.

On the basis of the aforementioned results and mechanistic pathways previously reported in the literature, we propose the mechanism depicted in Schemes 4 and S19–S21. The reaction sequence is initiated by a photo-induced electron-transfer process between boryl-anion-activated **1** (LG = X, O, or N) (**A**) and 2-PySNa/B_2pin_2 adduct **B** to afford the thiyl radical and radical anion of **1**.[74] In the case of **1j**, **1p**, and **1r**, EDA complexes were directly formed between substrates and thiolates (Schemes S19 and S20). Upon photoexcitation of the EDA complexes, an inner-sphere electron transfer occurs to arrive at the thiyl radical and radical anion of **1**.[75] The resulting radical anion undergoes cleavage of the C–LG bond to form the phenyl radical, which then reacts with a sp^3–sp^2 diboron species $[F\text{-}B_2pin_2]^-$ to give the desired borylation product **2a** and boryl radical anion **E**. Finally, the thiyl radical **C** is reduced by boryl radical anion **E** to regenerate thiolate, closing the catalytic cycle.

Conclusion

In summary, we have developed a new photocatalytic strategy for the *ipso*-borylation of substituted arenes by using thiolate as a catalyst. This strategy realized the borylation of a very broad range of inert C–X bonds, including non-activated C–F bonds, C–O bonds of phenol derivatives (carbonate, sulfamate, phosphate, and carbamate), C–N bonds of ammonium salts, and C–S bonds (sulfone, sulfoxide, and sulfide), with very negative reduction potentials, which are challenging via existing photoredox activation. In this manner, this system allows the utilization of a range of unconventional leaving groups for radical borylation reactions, thus expanding available substrate types to access arylboronates. Despite the generated high reducing power, this reaction displays broad functional-group tolerance and furnishes borylated products in moderate to excellent yields. We propose the formation of an EDA complex between thiolate/B_2pin_2 and boryl-anion-activated substrates as the key step in obtaining the reactivity, which is supported by UV-vis measurements, NMR analysis, and control experiments. This combination of photochemistry with thiolate catalysis constitutes a unique activation mode of substituted arenes in cross-coupling reactions. Further studies on the detailed reaction mechanism and the extension of this catalytic system to other coupling partners are currently underway in our laboratory.

EXPERIMENTAL PROCEDURES

Resource availability

Lead contact

Further information and requests for resources should be directed to and will be fulfilled by the lead contact, Burkhard König (burkhard.koenig@ur.de).

Materials availability

Unique and stable reagents generated in this study will be made available on request, but we might require a payment and/or a completed materials transfer agreement if there is potential for commercial application.

Data and code availability

There is no dataset or code associated with the paper.

Methods

Full experimental procedures are provided in the supplemental information.

SUPPLEMENTAL INFORMATION

Supplemental information can be found online at https://doi.org/10.1016/j.chempr.2021.04.016.

ACKNOWLEDGMENTS

This project received funding from the European Research Council under the European Union’s Horizon 2020 Research And Innovation Programme (grant agreement no. 741623). S.W. thanks the China Scholarship Council (CSC) for a predoctoral fellowship (CSC student no. 201606280052). We are grateful to Prof. Armido Studer (University of Münster) for helpful discussions. We further thank Dr. Rudolf Vasold (University of Regensburg) for his assistance in GC-MS measurements and Ms. Regina Hoheisel (University of Regensburg) for her assistance in cyclic voltammetry measurements.

AUTHOR CONTRIBUTIONS

B.K. supervised the project; S.W. developed the catalytic system, conducted the experiments, and analyzed the data; S.W. and H.W. conducted the mechanistic studies; and S.W. and B.K. wrote the manuscript with input from all of the authors.

DECLARATION OF INTERESTS

The authors declare no competing interests.

Received: December 1, 2020
Revised: February 24, 2021
Accepted: April 29, 2021
Published: May 28, 2021

REFERENCES

1. Xuan, J., and Xiao, W.J. (2012). Visible-light photoredox catalysis. Angew. Chem. Int. Ed. *51*, 6828–6838.
2. Narayanam, J.M.R., and Stephenson, C.R.J. (2011). Visible light photoredox catalysis: applications in organic synthesis. Chem. Soc. Rev. *40*, 102–113.
3. Prier, C.K., Rankic, D.A., and MacMillan, D.W.C. (2013). Visible light photoredox catalysis with transition metal complexes: applications in organic synthesis. Chem. Rev. *113*, 5322–5363.
4. Romero, N.A., and Nicewicz, D.A. (2016). Organic photoredox catalysis. Chem. Rev. *116*, 10075–10166.
5. Skubi, K.L., Blum, T.R., and Yoon, T.P. (2016). Dual catalysis strategies in photochemical synthesis. Chem. Rev. *116*, 10035–10074.
6. Marzo, L., Pagire, S.K., Reiser, O., and König, B. (2018). Visible-light photocatalysis: does it make a difference in organic synthesis? Angew. Chem. Int. Ed. *57*, 10034–10072.
7. Glaser, F., Kerzig, C., and Wenger, O.S. (2020). Multi-photon excitation in photoredox catalysis: concepts, applications, methods. Angew. Chem. Int. Ed. *59*, 10266–10284.
8. Ghosh, I., Marzo, L., Das, A., Shaikh, R., and König, B. (2016). Visible light mediated photoredox catalytic arylation reactions. Acc. Chem. Res. *49*, 1566–1577.
9. Majek, M., and Jacobi von Wangelin, A. (2016). Mechanistic perspectives on organic photoredox catalysis for aromatic substitutions. Acc. Chem. Res. *49*, 2316–2327.
10. Ghosh, I. (2019). Excited radical anions and excited anions in visible light photoredox catalysis. Phys. Sci. Rev. *4*, 0185–2017.
11. Ghosh, I., Ghosh, T., Bardagi, J.I., and König, B. (2014). Reduction of aryl halides by consecutive visible light-induced electron transfer processes. Science *346*, 725–728.
12. Giedyk, M., Narobe, R., Weiß, S., Touraud, D., Kunz, W., and König, B. (2020). Photocatalytic activation of alkyl chlorides by assembly-promoted single electron transfer in microheterogeneous solutions. Nat. Catal. *3*, 40–47.
13. Ghosh, I., and König, B. (2016). Chromoselective photocatalysis: controlled bond activation through light-color regulation of redox potentials. Angew. Chem. Int. Ed. *55*, 7676–7679.
14. Cowper, N.G.W., Chernowsky, C.P., Williams, O.P., and Wickens, Z.K. (2020). Potent reductants via electron-primed photoredox catalysis: unlocking aryl chlorides for radical coupling. J. Am. Chem. Soc. *142*, 2093–2099.
15. Kim, H., Kim, H., Lambert, T.H., and Lin, S. (2020). Reductive electrophotocatalysis: merging electricity and light to achieve extreme reduction potentials. J. Am. Chem. Soc. *142*, 2087–2092.
16. MacKenzie, I.A., Wang, L., Onuska, N.P.R., Williams, O.F., Begam, K., Moran, A.M., Dunietz, B.D., and Nicewicz, D.A. (2020). Discovery and characterization of an acridine radical photoreductant. Nature *580*, 76–80.
17. Schmalzbauer, M., Marcon, M., and König, B. (2021). Excited State Anions in Organic Transformations. Angew. Chem. Int. Ed. *60*, 6270–6292.
18. Liu, W., Li, J., Huang, C.-Y., and Li, C.-J. (2020). Aromatic chemistry in the excited state:facilitating metal-free substitutions and cross-couplings. Angew. Chem. Int. Ed. *59*, 1786–1796.
19. D.G. Hall, ed. (2011). Boronic Acids: Preparation and Applications in Organic Synthesis, Medicine and Materials, Second Edition (Wiley-VCH Press).
20. Miyaura, N., and Suzuki, A. (1995). Palladium-catalyzed cross-coupling reactions of organoboron compounds. Chem. Rev. *95*, 2457–2483.
21. Ishiyama, T., Murata, M., and Miyaura, N. (1995). Palladium(0)-catalyzed cross-coupling reaction of alkoxydiboron with haloarenes: a direct procedure for arylboronic esters. J. Org. Chem. *60*, 7508–7510.
22. Neeve, E.C., Geier, S.J., Mkhalid, I.A.I., Westcott, S.A., and Marder, T.B. (2016). Diboron(4) compounds: from structural curiosity to synthetic workhorse. Chem. Rev. *116*, 9091–9161.
23. Friese, F.W., and Studer, A. (2019). New avenues for C–B bond formation via radical intermediates. Chem. Sci. *10*, 8503–8518.
24. Nguyen, V.D., Nguyen, V.T., Jin, S., Dang, H.T., and Larionov, O.V. (2019). Organoboron chemistry comes to light: recent advances in photoinduced synthetic approaches to organoboron compounds. Tetrahedron *75*, 584–602.
25. Wang, M., and Shi, Z. (2020). Methodologies and strategies for selective borylation of C–Het and C–C Bonds. Chem. Rev. *120*, 7348–7398.
26. Yan, G., Huang, D., and Wu, X. (2018). Recent advances in C–B bond formation through a free radical pathway. Adv. Synth. Catal. *360*, 1040–1053.
27. Tian, Y.M., Guo, X.N., Braunschweig, H., Radius, U., and Marder, T.B. (2021). Photoinduced borylation for the synthesis of organoboron compounds. Chem. Rev. *121*, 3561–3597. https://doi.org/10.1021/acs.chemrev.0c01236.
28. Yu, J., Zhang, L., and Yan, G. (2012). Metal-free, visible light-induced borylation of aryldiazonium salts: a simple and green synthetic route to arylboronates. Adv. Synth. Catal. *354*, 2625–2628.
29. Ahammed, S., Nandi, S., Kundu, D., and Ranu, B.C. (2016). One-pot Suzuki coupling of aromatic amines via visible light photocatalyzed metal free borylation using t-BuONO at room temperature. Tetrahedron Lett. *57*, 1551–1554.
30. Lei, T., Wei, S.M., Feng, K., Chen, B., Tung, C.H., and Wu, L.Z. (2020). Borylation of diazonium salts by highly emissive and crystalline carbon dots in water. ChemSusChem *13*, 1715–1719.
31. Mfuh, A.M., Doyle, J.D., Chhetri, B., Arman, H.D., and Larionov, O.V. (2016). Scalable, metal- and additive-free, photoinduced borylation of haloarenes and quaternary arylammonium salts. J. Am. Chem. Soc. *138*, 2985–2988.
32. Jin, S., Dang, H.T., Haug, G.C., He, R., Nguyen, V.D., Nguyen, V.T., Arman, H.D., Schanze, K.S., and Larionov, O.V. (2020). Visible light-induced borylation of C–O, C–N, and C–X Bonds. J. Am. Chem. Soc. *142*, 1603–1613.
33. Chen, K., Zhang, S., He, P., and Li, P. (2016). Efficient metal-free photochemical borylation of aryl halides under batch and continuous-flow conditions. Chem. Sci. *7*, 3676–3680.
34. Jiang, M., Yang, H., and Fu, H. (2016). Visible-light photoredox borylation of aryl halides and subsequent aerobic oxidative hydroxylation. Org. Lett. *18*, 5248–5251.
35. Cheng, Y., Mück-Lichtenfeld, C., and Studer, A. (2018). Metal-free radical borylation of alkyl and aryl iodides. Angew. Chem. Int. Ed. *57*, 16832–16836.
36. Qiao, Y., Yang, Q., and Schelter, E.J. (2018). Photoinduced Miyaura borylation by a rare-earth-metal photoreductant: the hexachlorocerate(III) anion. Angew. Chem. Int. Ed. *57*, 10999–11003.
37. Zhang, L., and Jiao, L. (2019). Visible-light-induced organocatalytic borylation of aryl chlorides. J. Am. Chem. Soc. *141*, 9124–9128.
38. Tian, Y.M., Guo, X.N., Krummenacher, I., Wu, Z., Nitsch, J., Braunschweig, H., Radius, U., and Marder, T.B. (2020). Visible-light-induced Ni-catalyzed radical borylation of chloroarenes. J. Am. Chem. Soc. *142*, 18231–18242.
39. Tian, Y.M., Guo, X.N., Kuntze-Fechner, M.W., Krummenacher, I., Braunschweig, H., Radius, U., Steffen, A., and Marder, T.B. (2018). Selective photocatalytic C–F borylation of polyfluoroarenes by Rh/Ni dual catalysis providing valuable fluorinated arylboronate esters. J. Am. Chem. Soc. *140*, 17612–17623.
40. Liu, W., Yang, X., Gao, Y., and Li, C.J. (2017). Simple and efficient generation of aryl radicals from aryl triflates: synthesis of aryl boronates and aryl iodides at room temperature. J. Am. Chem. Soc. *139*, 8621–8627.
41. Nitelet, A., Thevenet, D., Schiavi, B., Hardouin, C., Fournier, J., Tamion, R., Pannecoucke, X., Jubault, P., and Poisson, T. (2019). Copper-photocatalyzed borylation of organic halides under batch and continuous-flow conditions. Chem. Eur. J. *25*, 3262–3266.
42. Candish, L., Teders, M., and Glorius, F. (2017). Transition-metal-free, visible-light-enabled decarboxylative borylation of aryl N-hydroxyphthalimide esters. J. Am. Chem. Soc. *139*, 7440–7443.
43. Schmalzbauer, M., Svejstrup, T.D., Fricke, F., Brandt, P., Johansson, M.J., Bergonzini, G., and König, B. (2020). Redox-neutral photocatalytic C−H carboxylation of arenes and styrenes with CO$_2$. Chem *6*, 2658–2672.

44. Schmalzbauer, M., Ghosh, I., and König, B. (2019). Utilising excited state organic anions for photoredox catalysis: activation of (hetero)aryl chlorides by visible light-absorbing 9-anthrolate anions. Faraday Discuss. *215*, 364–378.

45. Wang, S., Lokesh, N., Hioe, J., Gschwind, R.M., and König, B. (2019). Photoinitiated carbonyl-metathesis: deoxygenative reductive olefination of aromatic aldehydes via photoredox catalysis. Chem. Sci. *10*, 4580–4587.

46. Tobisu, M., Furukawa, T., and Chatani, N. (2013). Visible light-mediated direct arylation of arenes and heteroarenes using diaryliodonium salts in the presence and absence of a photocatalyst. Chem. Lett. *42*, 1203–1205.

47. Marzo, L., Wang, S., and König, B. (2017). Visible-light-mediated radical arylation of anilines with acceptor-substituted (hetero)aryl halides. Org. Lett. *19*, 5976–5979.

48. Liu, B., Lim, C.H., and Miyake, G.M. (2017). Visible-light-promoted C–S cross-coupling via intermolecular charge transfer. J. Am. Chem. Soc. *139*, 13616–13619.

49. Liang, K.J., Li, N., Zhang, Y., Li, T., and Xia, C.F. (2019). Transition-metal-free α-arylation of oxindoles via visible-light-promoted electron transfer. Chem. Sci. *10*, 3049–3053.

50. Li, G.Q., Yan, Q.L., Gan, Z.Y., Li, Q., Dou, X.M., and Yang, D.S. (2019). Photocatalyst-free visible-light-promoted C(sp^2)-S coupling: a strategy for the preparation of S-aryl dithiocarbamates. Org. Lett. *21*, 7938–7942.

51. Wu, J.J., Bär, R.M., Guo, L., Noble, A., and Aggarwal, V.K. (2019). Photoinduced deoxygenative borylations of aliphatic alcohols. Angew. Chem. Int. Ed. *58*, 18830–18834.

52. Schweitzer-Chaput, B., Horwitz, M.A., de Pedro Beato, E., and Melchiorre, P. (2019). Photochemical generation of radicals from alkyl electrophiles using a nucleophilic organic catalyst. Nat. Chem. *11*, 129–135.

53. Mazzarella, D., Magagnano, G., Schweitzer-Chaput, B., and Melchiorre, P. (2019). Photochemical organocatalytic borylation of alkyl chlorides, bromides, and sulfonates. ACS Catal. *9*, 5876–5880.

54. De Pedro Beato, E., Mazzarella, D., Balletti, M., and Melchiorre, P. (2020). Photochemical generation of acyl and carbamoyl radicals using a nucleophilic organic catalyst: applications and mechanism thereof. Chem. Sci. *11*, 6312–6324.

55. Spinnato, D., Schweitzer-Chaput, B., Goti, G., Ošeka, M., and Melchiorre, P. (2020). A photochemical organocatalytic strategy for the α-alkylation of ketones by using radicals. Angew. Chem. Int. Ed. *59*, 9485–9490.

56. Huang, H., Ye, J.-H., Zhu, L., Ran, C.-K., Miao, M., Wang, W., Chen, H., Zhou, W.-J., Lan, Y., Yu, B., and Yu, D.G. (2020). Visible-light-driven anti-Markovnikov hydrocarboxylation of acrylates and styrenes with CO$_2$. CCS Chem. *2*, 1746–1756.

57. Li, H.Y., Tang, X.X., Pang, J.H., Wu, X.Y., Yeow, E.K.L., Wu, J., and Chiba, S. (2021). Polysulfide anions as visible light photoredox catalysts for aryl cross-couplings. J. Am. Chem. Soc. *143*, 481–487.

58. McClain, E.J., Monos, T.M., Mori, M., Beatty, J.W., and Stephenson, C.R.J. (2020). Design and implementation of a catalytic electron donor–acceptor complex platform for radical trifluoromethylation and alkylation. ACS Catal. *10*, 12636–12641.

59. Chen, K., Cheung, M.S., Lin, Z., and Li, P. (2016). Metal-free borylation of electron-rich aryl (pseudo)halides under continuous-flow photolytic conditions. Org. Chem. Front. *3*, 875–879.

60. Zeng, H., Qiu, Z., Domínguez-Huerta, A., Hearne, Z., Chen, Z., and Li, C.-J. (2017). An adventure in sustainable cross-coupling of phenols and derivatives via carbon–oxygen bond cleavage. ACS Catal. *7*, 510–519.

61. Qiu, Z., and Li, C.J. (2020). Transformations of less-activated phenols and phenol derivatives via C–O cleavage. Chem. Rev. *120*, 10454–10515.

62. Kaiser, D., Klose, I., Oost, R., Neuhaus, J., and Maulide, N. (2019). Bond-forming and -breaking reactions at sulfur(IV): sulfoxides, sulfonium salts, sulfur ylides, and sulfinate salts. Chem. Rev. *119*, 8701–8780.

63. Gao, J., Feng, J., and Du, D. (2020). Shining light on C−S bonds: recent advances in C−C bond formation reactions via C−S bond cleavage under photoredox catalysis. Chem. Asian J. *15*, 3637–3659.

64. Huang, C., Feng, J., Ma, R., Fang, S., Lu, T., Tang, W., Du, D., and Gao, J. (2019). Redox-neutral borylation of aryl sulfonium salts via C–S activation enabled by light. Org. Lett. *21*, 9688–9692.

65. Maekawa, Y., Ariki, Z.T., Nambo, M., and Crudden, C.M. (2019). Pyridine-catalyzed desulfonative borylation of benzyl sulfones. Org. Biomol. Chem. *17*, 7300–7303.

66. Raviola, C., and Protti, S. (2019). Leaving groups in metal-free arylations: make your choice! Eur. J. Org. Chem. *2020*, 5292–5304.

67. Crisenza, G.E.M., Mazzarella, D., and Melchiorre, P. (2020). Synthetic methods driven by the photoactivity of electron donor–acceptor complexes. J. Am. Chem. Soc. *142*, 5461–5476.

68. Lima, C.G.S., de M. Lima, T., Duarte, M., Jurberg, I.D., and Paixão, M.W. (2016). Organic synthesis enabled by light-irradiation of EDA complexes: theoretical background and synthetic applications. ACS Catal. *6*, 1389–1407.

69. Cheng, W.M., Shang, R., Zhao, B., Xing, W.L., and Fu, Y. (2017). Isonicotinate ester catalyzed decarboxylative borylation of (hetero)aryl and alkenyl carboxylic acids through N-hydroxyphthalimide esters. Org. Lett. *19*, 4291–4294.

70. Nguyen, P., Dai, C., Taylor, N.J., Power, W.P., Marder, T.B., Pickett, N.L., and Norman, N.C. (1995). Lewis base adducts of diboron compounds: molecular structures of [B$_2$(cat)$_2$(4-picoline)] and [B$_2$(cat)$_2$(4-picoline)$_2$] (cat = 1,2-O$_2$C$_6$H$_4$). Inorg. Chem. *34*, 4290–4291.

71. Katsuma, Y., Asakawa, H., and Yamashita, M. (2018). Reactivity of highly Lewis acidic diborane(4) towards pyridine and isocyanide: formation of boraalkene–pyridine complex and Ortho-functionalized pyridine derivatives. Chem. Sci. *9*, 1301–1310.

72. Pietsch, S., Neeve, E.C., Apperley, D.C., Bertermann, R., Mo, F., Qiu, D., Cheung, M.S., Dang, L., Wang, J., Radius, U., et al. (2015). Synthesis, structure, and reactivity of anionic sp^2-sp^3 diboron compounds: readily accessible boryl nucleophiles. Chem. Eur. J. *21*, 7082–7098.

73. Pinet, S., Liautard, V., Debiais, M., and Pucheault, M. (2017). Radical metal-free borylation of aryl iodides. Synthesis *49*, 4759–4768.

74. EDA complex is proposed to be formed by the [F$^-$-B2pin2]-activated sulfones with 1-AdSNa.

75. Lu, J., Khetrapal, N.S., Johnson, J.A., Zeng, X.C., and Zhang, J. (2016). "π-Hole−π" interaction promoted photocatalytic hydrodefluorination via inner-sphere electron transfer. J. Am. Chem. Soc. *138*, 15805–15808.